Published in final edited form as:
Biopolymers. 2013 October ; 99(10): . doi:10.1002/bip.22315.

Solution Phase Conformation and Proteolytic Stability of Amide-Linked Neuraminic Acid Analogues

Jonel P. Saludes[1,2,*], **Travis Q. Gregar**[3,†], **I. Abrrey Monreal**[2], **Brandan M. Cook**[2], **Lieza M. Danan-Leon**[4,#], and **Jacquelyn Gervay-Hague**[1,*]

[1]Department of Chemistry, University of California Davis, One Shields Ave., Davis, California, 95616

[2]Department of Chemistry, Washington State University, Pullman, Washington, 99164

[3]Department of Chemistry, The University of Arizona, Tucson, Arizona, 85721

[4]Campus Mass Spectrometry Facility, University of California Davis, One Shields Ave., Davis, California, 95616

Abstract

Amide-linked homopolymers of sialic acid offer the advantages of stable secondary structure and increased bioavailability making them useful constructs for pharmaceutical design and drug delivery. Defining the structural characteristics that give rise to secondary structure in aqueous solution is challenging in homopolymeric material due to spectral overlap in NMR spectra. Having previously developed computational tools for heteroologomers with resolved spectra, we now report that application of these methods in combination with circular dichroism, NH/ND NMR exchange rates and nOe data has enabled the structural determination of a neutral, □amide-linked homopolymer of a sialic acid analogue called Neu2en. The results show that the inherent planarity of the pyranose ring in Neu2en brought about by the □,□conjugated amide bond serves as the primary driving force of the overall conformation of the homooligomer. This peptide surrogate has an excellent bioavailability profile, with half-life of ~12 hours in human blood serum, which offers a viable peptide scaffold that is resistant to proteolytic degradation. Furthermore, a proof-of-principle study illustrates that Neu2en oligomers are functionalizable with small molecule ligands using 1,3-dipolar cycloaddition chemistry.

Keywords

Sialic acid; Neu2en; NMR; circular dichroism; helical peptide; water-soluble scaffold; blood serum; proteolysis; 1,3-dipolar cycloaddition chemistry; Click chemistry

INTRODUCTION

Sugar amino acids (SAAs) are carbohydrates that possess amino and carboxylic acid groups. The duality of functional groups along with the rigid sugar pyran framework[1] and readily convertible hydroxyl groups makes SAAs versatile building blocks for polymerization. *N*-Acetylneuraminic acid (sialic acid; Neu5Ac: (**1**)) is a naturally occurring nine-carbon SAA that forms homopolymeric structures (**1b**) through glycosidic attachment on both mammalian and bacterial cells.[2] Neu5Ac is also a □amino SAA and can be considered as a

*To whom correspondence should be addressed: jgervayhague@ucdavis.edu, jonel.saludes@wsu.edu.
†Current address: 3M, 3M Center, St. Paul, Minnesota 55144
#Current address: Sutro Biopharma Inc., South San Francisco, California 94080

conformationally restricted surrogate of a dipeptide, with torsion angles determined by the actual ring conformation (**1**).[3,4] The rigid framework of Neu5Ac gives rise to regions of fluxional helicity in the polymeric structures that adorn mammalian and bacterial cell surfaces.

Research in the Gervay-Hague laboratory has focused on making physiologically stable surrogates of polymeric Neu5Ac by replacing the labile glycosidic linkage between the anomeric carbon and the C-8 hydroxyl with an amide linkage between the C-1 carboxyl and the C-5 amine. To that end, the synthesis and structural characterization of the first water soluble Neu5Ac-based oligomers with stable secondary structure was reported in 1997 (Figure 2a).[5] Analyses of circular dichroism (CD) studies were consistent with peptide folding and in combination with NMR studies indicated that a minimum of 4 residues were required for ordered structure, and further elongation to eight residues increased 2° structure stability. Subsequent studies revealed the same general trend using different Neu5Ac analogs (Figure 2b–2d),[6] particularly those derived from Neu2en (**2**–**10**).

The NMR spectra of the amide-linked oligomers were complicated by spectral overlap and a general lack of analytical tools made it impossible to determine the three-dimensional structures of the homopolymers. To address these deficiencies, the synthesis of heterooligomers composed of Neu2en (**2**) and glutamic acid was undertaken. Glutamic acid (Glu) was chosen in an effort to reintroduce carboxylic acids into the amide-linked oligomers to mimic the functionality of the glycosidically-linked oligomers. At the outset, it was not clear if the stereochemistry of Glu would impact the secondary structure or if the order of incorporation would matter. To probe these questions, four sets of oligomers containing alternating Neu2en/L-Glu and Neu2en/D-Glu, as well as the reversed order D-Glu/Neu2en and L-Glu/Neu2en were synthetically prepared and structurally defined.[7] Incorporation of 2 different amino acid building blocks gave rise to chemical shift dispersion in the NMR spectra allowing the assignment of residues that could not be distinguished in the homopolymers. Additionally, XPLOR-NIH was parameterized to include Neu2en in addition to naturally occurring amino acids. The combination of chemical shift resolution, coupling constant data and nuclear Overhauser (nOe) effects when analyzed in XPLOR-NIH allowed the three dimensional structure of the heterooligomers to be defined. The results of these studies indicated that stable secondary structure was reinforced in oligomers containing L-Glu and that the preferred order was L-Glu/Neu2en (**11**). Most importantly, the results showed that L-Glu/Neu2en (**11**) adopts a similar helical structure to **1b** albeit with half the number of carboxylic acids per turn. Equally important was the later study, which showed that L-Glu/Neu2en (**11**) is proteolytically stable under physiological conditions.[8]

The advances gained from the heterooligomer studies provided important NMR and computational tool that have now enabled structural reinvestigation of the homopolymers. The studies reported herein include the three-dimensional structure determination of a polysialic acid analog consisting of α-amide-linked homooligomers of Neu2en. Fmoc-Neu2en (**12**) was chosen as the building block because earlier studies indicated that polymers made from this molecule were the most stable and synthetically accessible.[6] Subsequent studies probed the proteolytic stability of the homooligomer in human blood serum. Finally, functionalization of the homooligomer using an azide/alkyne 1,3-dipolar cylcoaddition afforded a fluorescent analog demonstrating the feasibility of conjugation chemistry. These combined studies establish a foundation for understanding the factors that contribute to structural and physiological stability and aid the rational design of biologically relevant molecular scaffolds.

Results

Conformational Studies by Circular Dichroism

The solid phase peptide synthesis (SPPS) of compounds **2** – **9** using **12** and **13** as building blocks and employing the classical SPPS method was previously reported by Gervay and co-workers.[6] Structural studies began by investigating the circular dichroism (CD) of **2**–**9**. Samples were prepared in water and their spectra were recorded at 25 °C. Molar ellipticity ([ ]) values were divided by the number of amide residues in the peptide to normalize the contribution of each chromophore to the observed circular dichroism.[5] Figure 4a shows the CD spectra of **2**–**9** revealing the same peak and trough profiles that were observed in helical L-Glu/Neu2en hybrid peptide (**11**).[7] Starting with the monomer **2**, a general shape is presented in the spectrum with a minimum at 210 nm and a maximum at 240 nm, which is attributed to the , unsaturated amide linked to the caproamide. There is an increasing difference in peak (240 nm) to trough (210 nm) molar ellipticity values ([ ]) from the dimer through the octamer indicating increasing folding behavior with length. The dimer (**3**) minimum and maximum dramatically decreases and increases, respectively; this change is attributed to the increase in the number of inter-residue chromophores. The trimer (**4**) shows a larger increase and decrease relative to the dimer, while the jump to the tetramer (**5**), pentamer (**6**) and hexamer (**7**) is less pronounced. Homooligomers **5**–**7** all display similar spectra suggesting a common secondary structure. The heptamer **8** is more closely aligned to the profile of the trimer, which has been interpreted as a transitional flux.[5] Stable secondary structure is restored and even more pronounced in the octamer (**9**), which exhibits an even larger peak to trough difference. Table 1 summarizes the peak maxima and peak minima, the associated $_{max}$ and $_{min}$ for each oligomer, and their [ ]. One may conceive of comparing the circular dichroic properties of Neu2en homooligomers with those of -peptides to gauge the stability of their 2° structures, but the absence of the classical helical polypeptide trough at 222 nm in Neu2en oligomers precludes the standard comparison of ellipticity at $[ ]_{222}$[9] (n– * transitions of the -helix) or their ellipticity ratio R_2 ($[ ]_{222}/[ ]_{208}$)[10] with -peptides. However, comparison of $[ ]_{208}$ (– * transitions of the -helix) of peptide **9** (−9539 deg-cm^2-dmol^{-1}) with the value reported in the literature indicates that it is not as helical as poly(L-lysine) ($[ ]_{208}$ = −32,600 ± 4000 deg-cm^2-dmol^{-1}).[11] Nonetheless, the 2° structure stability of compounds **5**–**9** are comparable with our previously reported Neu2en heterooligomers[7] that are resistant to thermal denaturation even at 80 °C, a temperature whereby most -helical polypeptides would denature.

In order to have a handle for attaching a fluorescent probe, an azide-functionalized analog of **7** was also prepared. The azide was introduced at the -C of the caproamide linker of the new hexamer (**10**) to enable copper-catalyzed 1,3-dipolar azide alkyne cycloaddition ('Click' chemistry)[12] at a later stage. The SPPS synthesis of **10** also utilized Fmoc chemistry but, in contrast to previous SPPS of Neu2en homooligomers, **14** was introduced as the linker and microwave technology was used to effect shorter reaction times.[7] As shown in Figure 4b, this slight structural modification of the caproamide side chain did not alter the CD signature; the CD profile of **10** is almost identical to **7** with a consistent $_{max}$ and $_{min}$ of 241 and 211 nm, respectively. Furthermore, the calculated [ ] of **10** at 19,217 mdeg-cm^2-dmol^{-1} is close to that of **7** at 18,874 mdeg-cm^2-dmol^{-1} (Table 1), which is within an acceptable experimental error of <2%. These findings indicate that appending an azide at the -C of the linker does not affect the 2° structure of the peptide.

NMR NH/ND Exchange Studies

In proteins and peptides, the measurement of the rate of amide NH/ND exchange by ^{1}H NMR spectroscopy is used to demonstrate the presence of peptide folding due to intramolecular H-bonding.[13] The rate of decrease of the NH resonance peak integration due

to deuterium exchange from the solvent is correlated to the exchange rate and is used to calculate the NH half-life ($t_{1/2}$) following pseudo-first-order kinetics. Deuterium exchange studies were performed on compounds **3** – **9** in NaD_2PO_4 buffer in D_2O at pD = 3.0 and 277 K to slow the exchange to an observable rate on the NMR time scale. NaD_2PO_4 buffer was chosen because it is known that the exchange rates of amide protons are slowest at this low pD.[14] Under these experimental conditions, the -hydrogen of the caproamide linker was observable but the carboxamide hydrogens were not found in the first FID. The rapid exchange confirms that in aqueous solutions, the terminal amide of the homooligomers is fully exposed to the solvent and does not form intramolecular H-bond. The *C*-terminal Neu2en residue shows a distinct amide resonance peak; however, the amide H's of internal residues overlapped and could not be differentiated. Table 2 lists the $t_{1/2}$ corresponding to the amide NH/ND exchange rates. The general trends of the study indicate fast exchange of the caproamide and terminal amide protons with fairly consistent rates through the oligomer lengths. Exchange rates for the internal amide protons also show a consistent rate throughout the oligomer series with the exception of the dimer and hexamer. The lack of a general trend of exchange rates in relation to the oligomer length indicates a lack of participation of the amide protons in the formation of secondary structure and suggests other inherent structural features in Neu2en that may be responsible for stable secondary structure.

NMR Conformational Analysis of Amide-linked Neu2en (10)

Compound **10** was selected for extensive ^1H and 2-D homonuclear NMR studies at 298 K to assign all ^1H resonances. NMR characterization proved to be challenging because of close and overlapping ^1H NMR peaks, even with an 800 MHz frequency spectrometer. Initial NMR studies were performed on the dimer, trimer, and tetramer analogue of **10** to differentiate terminal and internal residue resonances and to facilitate the assignment for **10** (data not shown). This strategy was further assisted by previous reports on resonance assignments for amide-linked Neu2en oligomers[6,7] that helped distinguish between the downfield *N*-terminal olefinic H3-1 proton from the *C*-terminal H3-6. The characterization began with H (3.22–3.31) of N_3Lys-7 because it is an unambiguous aminomethylene, and the assignment was walked through the residue to completely assign the protons using homonuclear COSY. Next, Neu2en H3 was used as a reporter atom that distinguished Neu2en-1 (5.96) from Neu2en-6 (5.84). Each of these residues have unique, distinguishable sets of ^1H NMR resonance peaks and assignment of proton resonances was accomplished by separately walking through intraresidue connectivities of both terminal residues using homonuclear COSY. Some overlapping peaks could not be differentiated i.e. H3 (5.91), H4 (4.65), H5 (4.26), H6 (4.50), H7 (3.67), H8 (3.93), H9 (3.67), and H9 (3.88) of Neu2en-2 to -5, and three residues (Neu2en-3 to -5) show the same amide H resonance of 8.18 ppm. The similarity in the ^1H NMR resonances is indicative of the similar environment that these internal residues experience. In contrast, the amide H resonance (8.22) of the next to end residue, Neu2en-2, were differentiated based on initial studies of the tetramer analogue. This finding is suggestive that the internal repeat units in the Neu2en homooligomer adopt the same conformation, a structural property that was also found in -2,8-linked polysialic acids.[15]

ROESY spectra using WATERGATE solvent suppression[16] were recorded for **10** prepared in 9:1 H_2O/D_2O to retain the resonances of exchangeable amide H for the elucidation of its three-dimensional structure in an aqueous environment. Also found in **10** were the same ROESY correlations between the polyhydroxy side chain protons H-8 with backbone amide H and H-9 with the olefinic H-3 of the immediately preceding residue that were previously observed in **11**. A number of ROESY cross peaks were assigned for **10** that helped define the backbone conformation of the peptide. These interactions were found to be sequential and recurring throughout the chain (Figure 5a). ROESY cross peak integrations were

calibrated and used as distance restraints for solution phase calculations using restrained molecular and simulated annealing in XPLOR-NIH[17] following the topology and parameters that were established for **12** and **14**.[7] The effect of solvent and solvent screening of electrostatic energy function in XPLOR structure calculation was implemented using the $1/R$ dielectric option for the energy function in XPLOR-NIH.[7] The *phi* and *psi* dihedral angles were obtained from ab initio calculations[18] and measured values for **11**.[7] A total of 100 iterations of simulated annealing and molecular dynamics calculations were performed, the lowest energy structures without NOE violations were selected, averaged, and energy minimized. Figure 5b shows a bundle of low-energy NMR-derived structures of **10** calculated using XPLOR-NIH with NOE restraints from ROESY spectra. It shows a closely packed backbone, but the glycerol side chain shows a lot of flexibility and movement. Furthermore, the overlaid structures do not converge well at the N-terminal residue, which appears to be frayed. This may explain why the amide H of Neu2en-2 showed only one ROESY with the glycerol side chain of Neu2en-1. Figure 5c is the horizontal side view of the averaged and minimized structure of **10** from 19 low energy structures. This model is defined by 84 nOe's, and the calculated backbone rmsd of 0.982 Å and a 1.912 Å rmsd for non-H atoms indicate good convergence (Table 3). The two carboxamide H of the linker are oriented away from any H-bond acceptors, which accounts for their fast deuterium exchange. The azide is oriented outwards making it accessible for functionalization with relevant small molecule ligands by cycloaddition chemistry. The hydroxyl group on the allylic C-4 of Neu2en is also oriented away from the core of the helix, which also makes it a favorable site for chemical modification. The glycerol side chains of Neu2en residues are extended and could be easily solvated, which explains the high solubility of amide-linked sialooligomers. This is in contrast to the intractable and water-insoluble glucose-derived, amide-linked polymers reported by Fuchs and Lehmann that lack this polyhydroxy side chain.[19]

Further analysis of the model for **10** revealed a left-handed helix with a pitch of 18.8 Å and 3.5 residues per turn (n). This conformation is significantly different from the observations for **11**, which has a deep cleft in the helix and a shorter pitch of 7.4 Å and $n = 3.7$.[7] These structural differences can be attributed to the backbone and amide periodicity. Compound **10** is made of repeating pyranose rings of Neu2en and each residue is analogous to a dipeptide as shown for **1**.[3,4] The pyranose ring is flattened because of the conjugated □, □unsaturated amide bond that gives rise to a puckered conformation characteristic of a glycal, and a preferred *trans*-□amide bonds with the amide H *cis* to the ring *O*. Therefore, one complete helical turn of **10** has three amide bonds but contains an equivalent of seven □-amino acid residues. In contrast, the helix in **11** contains a sum of three □and □amide bonds at an equivalent of six □-amino acid residues, and the □-amide bond further contributes to the shorter turn of this helix.

A comparison of the conformations off **10** and **11** shown in Figure 6 reveals opposite handedness of these oligomers and pronounced difference in the depth of the cleft, with **10** possessing a shallow cleft and a wider helical turn that has a pitch 2.5 times longer than **11**. The combination of ring conformation and a longer peptide backbone accounts for the difference in the 2° structures of **10** and **11**. By way of comparison to peptides, the poly-L-Ala-containing segment of T4 lysozyme[20] (pdb: 1L64) is an □-helical peptide. The model of **10** when compared with 1L64 (39–50) shows that although their n is almost the same, it requires 3.5 □-helices (11.5 residues) to equal the length of one full turn of **10** (Figure 6). Although pyranose SAA's could theoretically represent the length of a dipeptide and one helix of **10** is calculated to be equivalent to seven □-amino acid residues, the extended helical shape of **10** renders this molecule longer. The extended conformation also explains the rapid NH/ND exchange found in **2**–**9** because the amide H in the peptide backbone is readily accessible for deuterium exchange.

The structural characteristics of **10** provide essential information for the future design on Neu5Ac-derived peptide scaffolds. Since the extended homooligomer conformation is defined by restricted motion about the Neu2en glycal and preferred conformation of the amide, modifications of the sugar hydroxyl groups should not alter the 2° structure offering the advantage of further manipulation on **12** prior to peptide synthesis. The allylic C-4 hydroxyl could be replaced by an azide or guanidinium group, followed by further functionalization with small molecules as we have previously demonstrated.[21] Modifications on the pendant glycerol side chain present another potential of incorporating small molecule ligands without concern on the attenuation of the solubility of Neu2en homooligomers since it has been shown that transformations at this site do not affect water solubility of sialic acid derivatives.[22,23]

Proteolytic Stability in Human Blood Serum

Short peptides are labile towards proteolytic enzymes. From the perspective of pharmaceutical development, the degradative action of proteases on proteins and peptides presents a significant hurdle, and is a major impediment towards drug development.[24] Structural modifications employing D-isomers or extending the peptide backbones with amino acids have been employed to prolong metabolic half-life ($t_{1/2}$) and increase stability.[25,26] *In vitro* incubation closely reproduces the proteolytic activity in the blood and provides a good estimation of *in vivo* metabolism.[27] We previously reported the proteolytic resistance of Neu2en-derived /-hybrid peptide towards degradation by endogenous human blood proteases in human blood plasma.[11] This study was performed using radiometal-DOTA labeling and cellulose acetate electrophoresis (CAE), which revealed $t_{1/2}$ that are two- to three-orders of magnitude higher than natural -peptides.

The stability profile of **10** was studied in the presence of human blood serum with the aim of investigating the resistance of amide-linked sialic acid homooligomers towards peptide processing. Blood serum contains serine proteases, which are inactivated in plasma preparations, that contribute to the total enzymatic activity of all proteases found in the blood and mimic the physiological environment. Proteolytic stability was studied using HPLC-MS, a radiolabel-free, environmentally-friendly, and less-hazardous technique than the radiometal-DOTA-CAE method. Compound **10** was incubated in the blood serum at 37 °C, samples were taken at 0, 2, 4, 8, 16 h, and the serum proteins were precipitated. The supernatant was analyzed by HPLC coupled to ESI-MS at SIM mode to selectively detect the *m*/*z* due to **10** and eliminate interference from the matrix. The peak area at each time point was integrated and the serum $t_{1/2}$ was calculated using the least squares analysis of the integration peaks *vs.* time following pseudo-first-order kinetics.[28,29] Figure 7 is the pseudo-first-order rate plot showing that **10** has $t_{1/2}$ = 11.7 h. This result indicates that **10** persists for a long time in the presence of a mixture of at least 25 known amino- and carboxypeptidases found in the blood,[25] and possesses a $t_{1/2}$ of about fifty times more than those of natural -peptides.[30]

Investigations on the proteolytic resistance of unnatural peptides over the past decade have employed isolated enzymes[31–36] or animal serum[33], and only two recent reports utilized human blood components.[8,37] For example, the $t_{1/2}$ of hybrid /-peptide mimics of Bcl-x_L is ~9 to >1200 min in isolated enzymes and 820 to >2200 min in 50% fetal bovine serum.[33] The $t_{1/2}$ of **10** is shorter when compared to the proteolytic resistance of In-labeled DOTA conjugate of L-Glu/Neu2en **11**.[11] We explain this discrepancy as due to the difference in the 2° structures of **10** and **11**: the former has an extended conformation and more accessible amide bonds while the latter has a deeper cleft and a tighter wound helix. The C=O---H-N H-bonding observed in **11** that is not found in **10** contributes to the 2° structure and proteolytic stability of **11**. Nonetheless, the $t_{1/2}$ of **10** is significantly longer than what has

been observed *in vivo* in mice for a 15-mer α-2,8-*O*-linked Neu5Ac (90% degraded in 30 min), [38] which further proves the point that amide-linked Neu2en oligomers are more resistant towards enzymatic degradation than polysialic acid.

Neu2en Oligomer is Functionalizable at the *C*-terminus by 'Click' Chemistry

In previous work, we alluded to the use of the *C*-terminal α-azido moiety of the Neu2en-based peptides as a handle for scaffold conjugation.[7] In our proof-of-principle study, attempts to conjugate an alkyne functionalized small molecule to the homooligomer **10** by 'Click' chemistry to yield **16** (Figure 8) proved successful. N-(7-Nitro-2,1,3-benzoxadiazol-4-yl)-N-(2-propynyl)amine (NBD-propargylamine, **15**) was selected as a small molecule model because this compound is fluorogenic and is an excellent probe for studying the interactions of peptides with macromolecular systems like proteins and phospholipid vesicles.[39,40]

Following our reported method,[41] compound **16** was prepared by solution phase copper-catalyzed cycloaddition chemistry using tris[(1-benzyl-1H-1,2,3-triazol-4-yl)methyl]amine as ligand and an excess amount of Cu(I) in the form of $[(CH_3CN)_4Cu]PF_6$ that did not require sodium ascorbate for the regeneration of Cu(I) species. This method is advantageous because copper/sodium ascorbate mixture has been shown to be detrimental to biological and synthetic polymers. The crucial step in our approach is the efficient degassing of the solvents with N_2 for at least 30 min to ensure the removal of dissolved O_2. This method was found to be convenient and straightforward and yielded compound **16** after 25 h at room temperature. Although the reaction was sluggish, this demonstrates the proof-of-principle that Neu2en oligomers have the potential as metabolically-stable scaffolds for small molecule ligand display. We are currently investigating other ligands to help accelerate the kinetics of this reaction.

Conclusions

Reported herein for the first time is the three-dimensional 2° structural determination of a β-amide-linked homooligomer of the *N*-acetylneuraminic acid derivative Neu2en in water using a combination of spectroscopic and computational tools that have been developed. The stability of the helix increases with length as observed in the increase in the difference in their [θ] in CD. The important features in the 2° structure of **10** include the fact that the α-azido group does not perturb the helix, the observation of nOe's of the H's in the polyhydroxy side chains with the amide backbone, and the inherent planarity of the pyranose ring effected by the π,π-conjugated amide bond that serves as the driving force of the overall conformation of the peptide. Furthermore, this work also demonstrates the proof-of-principle that amide-linked sialic acid oligomers could be decorated with small molecule alkynes at the ω-C azide of the caproamide linker. The findings show that amide-linked Neu2en homooligomers represent novel scaffolds that provide a stable backbone that has potential for manipulation at the C-4 position, glycerol side chain, and ω-azido moiety. Future studies will be directed toward the replacement of the hydroxyl groups with other chemical handles and the development of improved synthetic protocols for scaffold functionalization.

Experimental Section

Experimental procedures for the synthesis of compounds **2–10** and **14** have been fully described elsewhere.[6,7]

Solid Phase Peptide Synthesis

Typically, 100 mg of dry Fmoc-Rink resin (0.5 mmol/g) was taken, swelled in DMF for 2 h, and drained. The classical, room temperature SPPS and purification of compounds **2** – **9** was previously reported.[6] Microwave-assisted SPPS, monitoring, and cleavage from solid support of **10** followed the previously reported method[7] using either CEM Discover or Biotage Initiator+ SP Wave peptide synthesizer. Microwave conditions are as follows: power = 20 W, ramp time = 2 min, hold time = 5 min, temperature = 75 °C. The crude peptide was purified by reverse phase HPLC (RP-C_{18}, 10 x 250 mm; 5–35% aqueous MeCN with 0.1% TFA) with detection set at 225 and 260 nm. Eluates were concentrated and lyophilized to yield white, fluffy solid TFA salt of the peptide.

Compound **10:** This was obtained in 22% purified yield. ^{1}H NMR (D_2O, 800 MHz): □5.96 (d, 1H, *J* = 3.0 Hz, H3-1), 5.91 (d, 4H, *J* = 1.8 Hz, H3-2/3/4/5), 5.84 (d, 1H, *J* = 1.8 Hz, H3-6), 4.65-4.64 (m, 4H, H4-2/3/4/5), 4.639-4.632 (m, 1H, H4-1), 4.636-4.628 (m, 1H, H4-6), 4.62 (d, 1H, *J* = 10.8 Hz, H6-1), 4.50 (d, 4H, *J* = 10.8 Hz, H6-2/3/4/5), 4.46 (d, 1H, *J* = 10.8 Hz, H6-6), 4.263 (dd, 1H, *J* = 10.8, 9.0 Hz, H5-2), 4.257 (dd, 3H, *J* = 10.8, 9.6 Hz, H5-3/4/5), 4.24 (dd, 1H, *J* = 11.4, 9.6 Hz, H5-6), 4.13 (dd, 1H, *J* = 7.2, 5.4 Hz, H □-7), 3.99 (ddd, 1H, *J* = 8.4, 5.4, 3.0 Hz, H8-1), 3.94 (ddd, 1H, *J* = 8.4, 5.4, 3.0 Hz, H8-2), 3.94-3.91 (m, 4H, H8-3/4/5/6), 3.904-3.898 (m, 1H, H7-1), 3.890-3.886 (m, 1H, H9 □1), 3.88-3.86 (m, 4H, H9 □3/4/5/6), 3.857-3.852 (m, 1H, H9 □2), 3.75 (dd, 1H, *J* = 12.0, 6.0 Hz, H9-1), 3.70-3.65 (m, 10H, H7/9-2/3/4/5/6), 3.64 (dd, 1H, *J* = 9.6, 8.4 Hz, H5-1), 3.37-3.28 (m, 2H, H □-7), 1.88-1.77 (m, 2H, H □-7), 1.64-1.58 (m, 2H, H □-7), 1.44 (p, 2H, *J* = 7.8 Hz, H □-7). ^{1}H NMR (9:1 H_2O/D_2O, 800 MHz): □8.22 (d, 1H, *J* = 8.8 Hz, HN5-2), 8.18 (d, 3H, *J* = 8.8 Hz, HN5-3/4/5), 8.17 (d, 1H, *J* = 7.2 Hz, HN5-6). ^{13} C NMR (D_2O, 150 MHz): □178.5, 167.2, 166.6, 166.1, 148.7, 148.5, 148.3, 111.8, 110.9, 79.1, 79.0, 77.9, 72.8, 70.6, 70.0, 67.5, 65.9, 65.8, 65.3, 53.7, 52.9, 41.9, 33.8, 30.7, 24.8. ESI-HRMS: [M + H^+] calcd for $C_{60}H_{92}N_{11}O_{37}^+$, 1558.5650; found, 1558.5816. [M + Na^+] calcd for $C_{60}H_{91}N_{11}O_{37}Na^+$, 1580.5470; found, 1580.5631. FT-IR (ATR, neat): 3306, 2114, 1668, 1642, 1535 cm^{-1}.

Circular Dichroism

Samples were prepared in water at a concentration of 0.5 to 1.0 mg/mL. Spectra were recorded in a 1 or 2 mm path length quartz cuvette at 25 °C. Three to five scans were obtained and averaged for each sample from 320 – 190 nm with data points taken every 1.0 nm. The values obtained form the raw data were used to calculate the molar ellipticity values [□], using the equation [□] = (□*M*)/(*cl*) where □is the corrected value, *M* is the molecular weight, *c* is the concentration in mg/mL, and *l* is the path length in mm. All molar ellipticity values were normalized per residue by dividing [□] by the number of amino acid residues in the oligomer.

Amide NH/ND Exchange

Samples were prepared in 25 mM NaD_2PO_4 buffer in D_2O at 0.01 M concentrations that was pre-cooled in an ice bath prior to addition to the peptides. ^{1}H NMR spectra were collected on a 600 MHz NMR spectrometer at 277 K using standard Bruker kinetics program. A total of 85 FIDs were obtained at 16 scans each with 8192 data points for a total acquisition time of 30 sec per FID. Integral areas were measured with normalization to a peak in the spectra not exchanging with D_2O. Data were processed, plotted the time versus integral area, fitted with an exponential curve, the half-life was calculated following pseudo-first order kinetics, and the plots are shown in the Supporting Information.

ROESY NMR and Solution Phase Structure Calculations

Compound **10** was dissolved in 0.5 mL of H_2O/D_2O (9:1) at a concentration of 1.1 mM, pH 6.0. All ROESY experiments were performed at 298 K on an 800 MHz spectrometer equipped with a 5 mm cryoprobe. Water suppression was achieved by WATERGATE technique.[16] ROESY spectra were recorded at 300 and 500 ms mixing times, and we found 300 ms to be optimal. All data were recorded using Bruker TopSpin and the ROESY cross-peak volumes in the contour plot were measured using Mestrenova software. Distance restraints, parameter and topology files, and restrained molecular dynamics and simulated annealing calculations were performed using the protocol of XPLOR-NIH as previously described.[7,17] The values for *phi* (190 ±30) and *psi* (180 ±40) dihedral angle restraints were obtained from *ab initio* calculations[18] and our previous report.[7] Visualization was done using MacPyMOL.[42 LLC. #1432]

Proteolytic Stability in Human Blood Serum

To 45 μL aliquots of human blood serum from a commercial source was added 5 μL solution of **10** (1.6 mg/mL) to give a final concentration of 100 μm. The mixture was vortex mixed and incubated at 37 °C. The samples were removed from the incubator at predetermined time points of 0, 2, 4, 8, and 16 h, and three replicates were setup for each time point. The serum proteins were precipitated using 50 μL MeOH, the mixture was cooled in an ice bath for 30 min, and centrifuged for 10 min at 16,000 x g. The supernatant was transferred to a polypropylene tube, the pellet was washed with 100 μL 50% aqueous MeOH, the wash was added to the supernatant, and the mixture was lyophilized. The dried mixture from the lyophilizer was taken up in 100 μL H_2O and centrifuged for 10 min at 16,000 x g. The supernatant was analyzed by RP-C_{18} HPLC (1.0 x 150 mm) at 0 – 10% for 10 min, 10 – 35% for 15 min, and 35 – 100% for 10 min MeCN in H_2O with 0.1% FA on a divert mode for the first 5 min. Detection was done using ESI-MS at SIM mode with masses set at *m*/*z* 1579–1585 $[(M+Na)]^+$, 1557–1563 $[(M+H)]^+$, 801–804 $[(M+Na2)]^{2+}$, and 790–793 $[(M+H+Na)]^{2+}$. Compound **10** eluted at 14.1 min. The peak area at each time point was integrated, the replicates averaged, and the serum half-life was calculated using the least squares analysis of the integration peaks *vs.* time following pseudo-first-order kinetics.[11]

Synthesis of N-(7-Nitro-2,1,3-benzoxadiazol-4-yl)-N-(2-propynyl)amine (15)

Compound **15** was prepared following a previous method[43] but with slight modifications. To a solution of NBD-Cl (250 mg, 1.25 mmol) dissolved in anhydrous MeCN (10 mL) was added propargylamine (138 mg, 2.5 mmol). The reaction mixture was kept under an inert atmosphere using Ar and stirred for 1 h at 0 °C, then allowed to warm to r.t. and reaction stirred for another 1 h. The solvent was evaporated under vacuum and the crude product purified by column chromatography using 2:1 hexane/EtOAc to afforded **15** (248 mg, 91% yield) as a brown powder. The ^{1}H NMR spectroscopic and mass spectrometric data were in agreement with the literature.[43]

Fluorophore conjugation by 'Click' chemistry

Peptide **16** was prepared using our previously published method.[41] To peptide **10** (14.8 mg, 12.5 μmol) was added N-(7-Nitro-2,1,3-benzoxadiazol-4-yl)-N-(2-propynyl)amine (**15**, 4.3 mg, 18.8 μmol) and the mixture taken up in 150 μL MeOH that was purged with N_2 for at least 30 min. To this mixture was added Tris[(1-benzyl-1H-1,2,3-triazol-4- yl)methyl]amine (TBTA, 19.9 mg, 37.5) and Tetrakis (acetonitrile)copper(I) hexafluorophosphate ($[(CH_3CN)_4Cu]PF_6$, 70.8 mg, 187.5 μmol). MeCN was added dropwise to bring everything into solution, and the reaction was allowed to proceed at room temperature with constant stirring for 25 h. The sample was quenched with 1 mL H_2O, frozen, and lyophilized to dryness. The dried crude product was re-suspended in 0.1 M EDTA, loaded on a Sep-Pak

C_{18} cartridge, and sequentially eluted with 5 mL of H_2O, 1:1 H_2O/MeCN, and MeCN. The H_2O/MeCN fraction was concentrated to dryness, dissolved in water, frozen, lyophilized to dryness to yield a yellow, fluffy solid TFA salt of **16.** ESI-MS: [M + Na^+] calcd for $C_{69}H_{97}N_{15}NaO_{40}^+$, 1798.6; found, 1799.1.

Supplementary Material

Refer to Web version on PubMed Central for supplementary material.

Acknowledgments

J.G.H. was supported by NSF Grant CHE-0518010 (UC Davis) and CHE-0196482 (U Arizona). J.P.S. is supported by Washington State University Startup Grant. Funding for the NMR spectrometers used in this project are acknowledged: UC Davis (NSF Grants CHE-0443516 and DBI-0722538), University of Arizona (NSF Grant OSTI 97-24412 and NIH Grant RR11973), and Washington State University (NIH grants RR0631401 RR12948, NSF grants CHE-9115282 and DBI-9604689 and the Murdock Charitable Trust).

References

1. Von Roedern EG, Kessler H. Angew Chem Int Ed Engl. 1994; 33:687–689.
2. Varki A. Trends Mol Med. 2008; 14:351–360. [PubMed: 18606570]
3. Von Roedern EG, Lohof E, Hessler G, Hoffmann M, Kessler H. J Am Chem Soc. 1996; 118:10156–10167.
4. Baldauf C, Gunther R, Hofmann HJ. J Org Chem. 2004; 69:6214–6220. [PubMed: 15357578]
5. Szabo L, Smith BL, McReynolds KD, Parrill AL, Morris ER, Gervay J. J Org Chem. 1998; 63:1074–1078.
6. Gregar TQ, Gervay-Hague J. J Org Chem. 2004; 69:1001–1009. [PubMed: 14961647]
7. Saludes JP, Ames JB, Gervay-Hague J. J Am Chem Soc. 2009; 131:5495–5505. [PubMed: 19323529]
8. Saludes JP, Natarajan A, DeNardo SJ, Gervay-Hague J. Chem Biol Drug Des. 2010; 75:455–460. [PubMed: 20486931]
9. Lazo ND, Downing DT. Biochemistry. 1997; 36:2559–2565. [PubMed: 9054562]
10. Bruch MD, Dhingra MM, Gierasch LM. Proteins: Struct, Funct, Genet. 1991; 10:130–139. [PubMed: 1896426]
11. Greenfield N, Fasman GD. Biochemistry. 1969; 10:4108–4116. [PubMed: 5346390]
12. Kolb HC, Finn MG, Sharpless KB. Angew Chem Int Ed. 2001; 40:2004–2021.
13. Appella DH, Christianson LA, Karle IL, Powell DR, Gellman SH. J Am Chem Soc. 1996; 118:13071–13072.
14. Wuthrich K, Wagner G. J Mol Biol. 1979; 130:1–18. [PubMed: 38342]
15. Brisson JR, Baumann H, Imberty A, Perez S, Jennings HJ. Biochemistry. 1992; 31:4996–5004. [PubMed: 1376145]
16. Piotto M, Saudek V, Sklenar V. J Biomol NMR. 1992; 2:661–665. [PubMed: 1490109]
17. Schwieters CD, Kuszewski JJ, Tjandra N, Clore GM. J Magn Reson. 2003; 160:65–73. [PubMed: 12565051]
18. Gregar, TQ. PhD Dissertation. The University of Arizona; Tucson: 2001.
19. Fuchs EF, Lehmann J. Carbohyd Res. 1976; 49:267–273.
20. Heinz DW, Baase WA, Matthews BW. Proc Natl Acad Sci USA. 1992; 89:3751–3755. [PubMed: 1570293]
21. Lu Y, Gervay-Hague J. Carbohydr Res. 2007; 342:1636–1650. [PubMed: 17597592]
22. Honda T, Masuda T, Yoshida S, Arai M, Kobayashi Y, Yamashita M. Bioorg Med Chem Lett. 2002; 12:1921–1924. [PubMed: 12113809]
23. Honda T, Yoshida S, Arai M, Masuda T, Yamashita M. Bioorg Med Chem Lett. 2002; 12:1929–1932. [PubMed: 12113811]

24. Manning MC, Patel K, Borchardt RT. Pharm Res. 1989; 6:903–918. [PubMed: 2687836]
25. Werle M, Bernkop-Schnurch A. Amino Acids. 2006; 30:351–367. [PubMed: 16622600]
26. Adessi C, Soto C. Curr Med Chem. 2002; 9:963–978. [PubMed: 11966456]
27. Falciani C, Lozzi L, Pini A, Corti F, Fabbrini M, Bernini A, Lelli B, Niccolai N, Bracci L. Chem Biol Drug Des. 2007; 69:216–221. [PubMed: 17441908]
28. Powell MF, Stewart T, Otvos L, Urge L, Gaeta FCA, Sette A, Arrhenius T, Thomson D, Soda K, Colon SM. Pharm Res. 1993; 10:1268–1273. [PubMed: 8234161]
29. Fernandes AI, Gregoriadis G. Biochim Biophys Acta. 1997; 1341:26–34. [PubMed: 9300806]
30. Powell MF. Annu Rep Med Chem. 1993; 28:285–294.
31. Frackenpohl J, Arvidsson PI, Schreiber JV, Seebach D. ChemBioChem. 2001; 2:445–455. [PubMed: 11828476]
32. Disney MD, Hook DF, Namoto K, Seeberger PH, Seebach D. Chem Biodiv. 2005; 2:1624–1634.
33. Sadowsky JD, Murray JK, Tomita Y, Gellman SH. ChemBioChem. 2007; 8:903–916. [PubMed: 17503422]
34. Seebach D, Abele S, Schreiber JV, Martinoni B, Nussbaum AK, Schild H, Schulz H, Hennecke H, Woessner R, Bitsch F. Chimia. 1998; 52:734–739.
35. Hook DF, Bindschadler P, Mahajan YR, Sebesta R, Kast P, Seebach D. Chem Biodiv. 2005; 2:591–632.
36. Schmitt MA, Weisblum B, Gellman SH. J Am Chem Soc. 2007; 129:417–428. [PubMed: 17212422]
37. Ahmed S, Kaur K. Chem Biol Drug Des. 2009; 73:545–552. [PubMed: 19317848]
38. Gregoriadis G, McCormack B, Wang Z, Lifely R. FEBS Lett. 1993; 315:271–276. [PubMed: 8422917]
39. Morton LA, Yang H, Saludes JP, Fiorini Z, Beninson LA, Chapman ER, Fleshner M, Xue D, Yin H. ACS Chem Biol. 2013; 8:218–225. [PubMed: 23075500]
40. Saludes JP, Morton LA, Ghosh N, Beninson L, Chapman ER, Fleshner M, Yin H. ACS Chem Biol. 2012; 7:1629–1635. [PubMed: 22769435]
41. Saludes JP, Morton LA, Coulup SK, Fiorini Z, Cook BM, Beninson L, Chapman ER, Fleshner M, Yin H. Mol BioSyst. 201310.1039/C3MB70109C
42. The PyMOL Molecular Graphics System, Version 1.3r1. Schrödinger, LLC;
43. Key JA, Cairo CW. Dyes Pigm. 2011; 88:95–102.

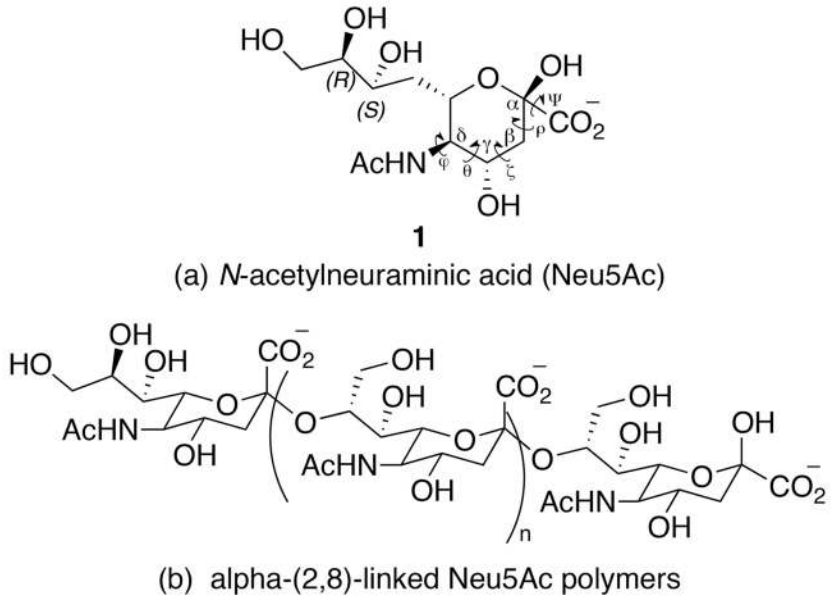

Figure 1.
N-acetylneuraminic acid and its *O*-linked homopolymers.

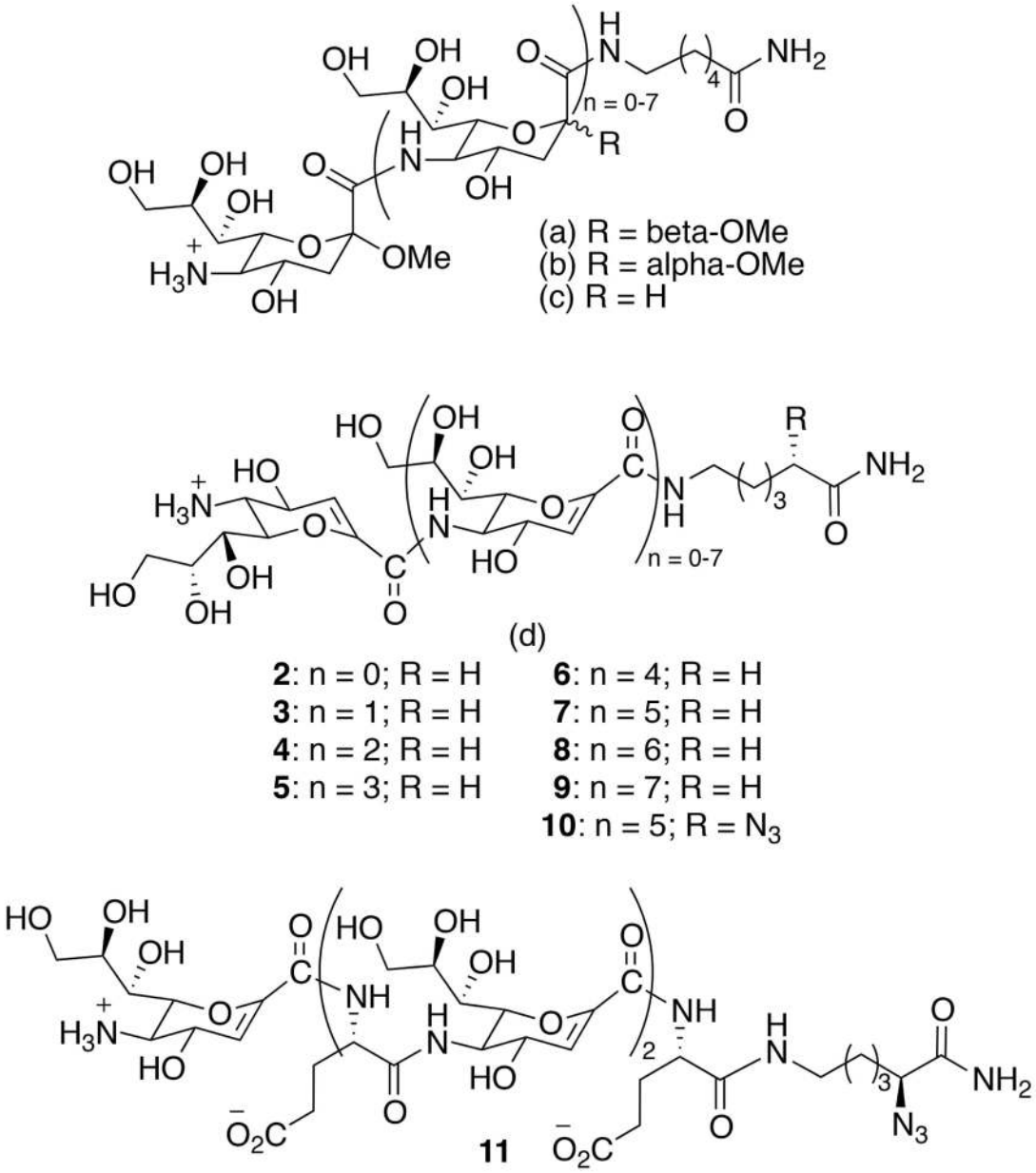

Figure 2.
Synthetic amide-linked homopolymers of *N*-acetylneuraminic acid derivatives.

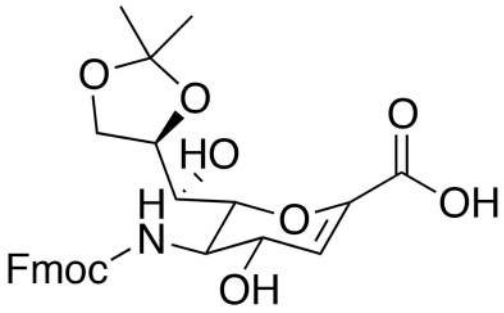

12

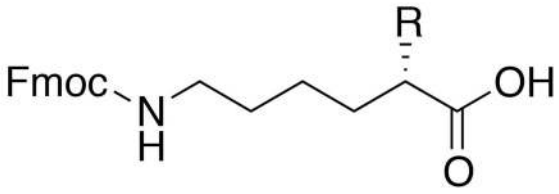

13: R = H
14: R = N_3

Figure 3.
Amino acids used for constructing the azide-functionalized amide-linked Neu2en.

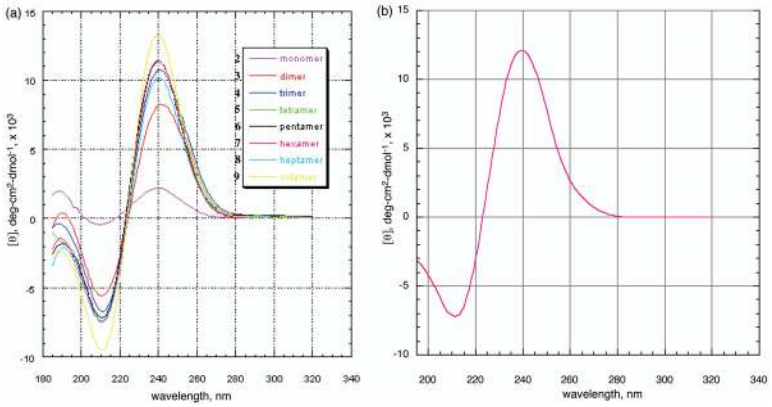

Figure 4.

(a) CD spectra of **2 – 9** at 25 °C showing the unique spectral signature of amide-linked Neu5Ac analogs. (b) CD spectrum of **10** at 25 °C showing a similar profile and consistent θ_{max} and θ_{min} with **7**, indicating that the presence of the azide moiety at the α-C of the linker does not affect peptide folding.

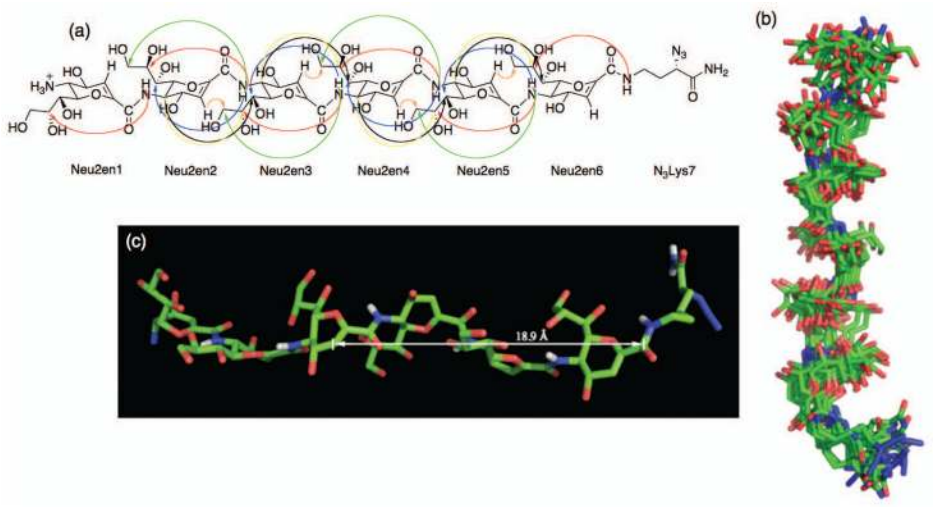

Figure 5.

(a) Crucial inter-residue long-range NOEs for **10** extracted from the ROESY spectra (9:1 H_2O/D_2O, 500 ms mixing time, 800 MHz, 298 K). (b) A bundle of low-energy NMR-derived structures of **10** calculated using XPLOR-NIH using NOE restraints from ROESY spectra. (c) Side view of the averaged and minimized solution phase structure of **10** showing an extended, left-handed helix (H atoms were omitted except the amide H).

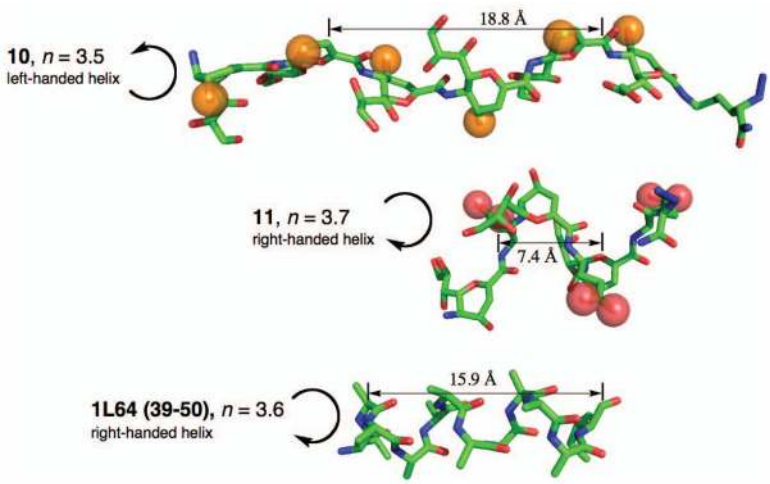

Figure 6.
Comparison of the conformations of **10** with **11** and 1L64 (39–50) (H atoms were omitted for clarity). Red spheres indicate O atoms of carboxylate groups while orange spheres indicate O atoms of hydroxyl groups at position 4 of Neu2en.

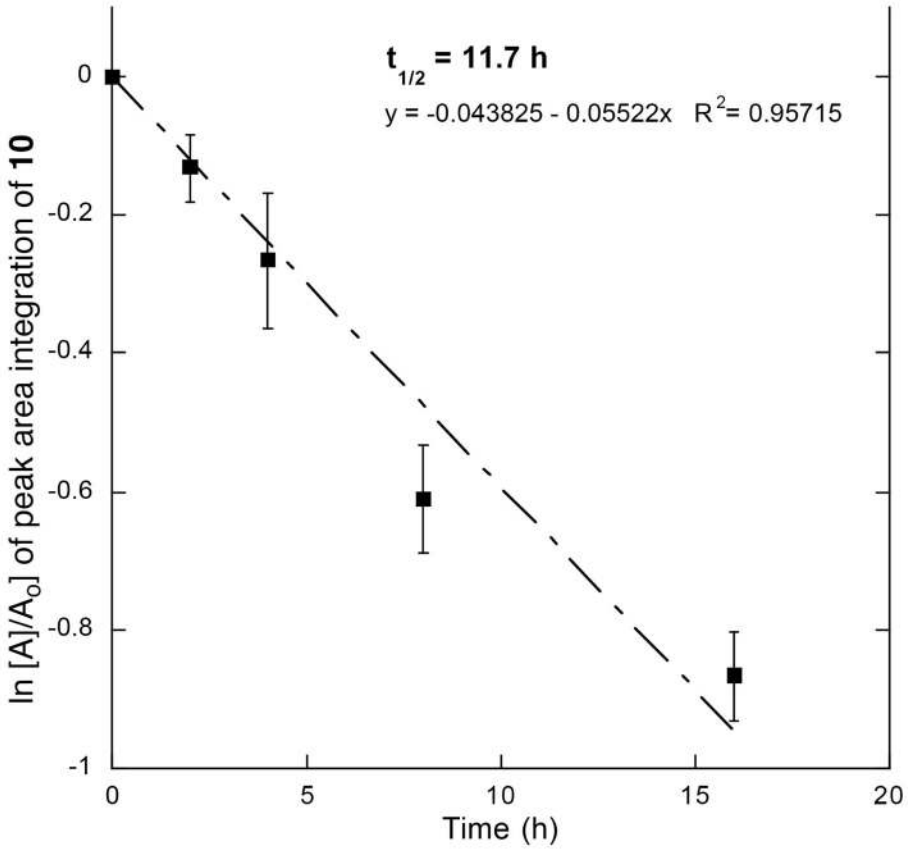

Figure 7.
Pseudo-first-order rate plot of the stability profile of **10** in human blood serum showing its $t_{1/2}$ of 11.7 h.

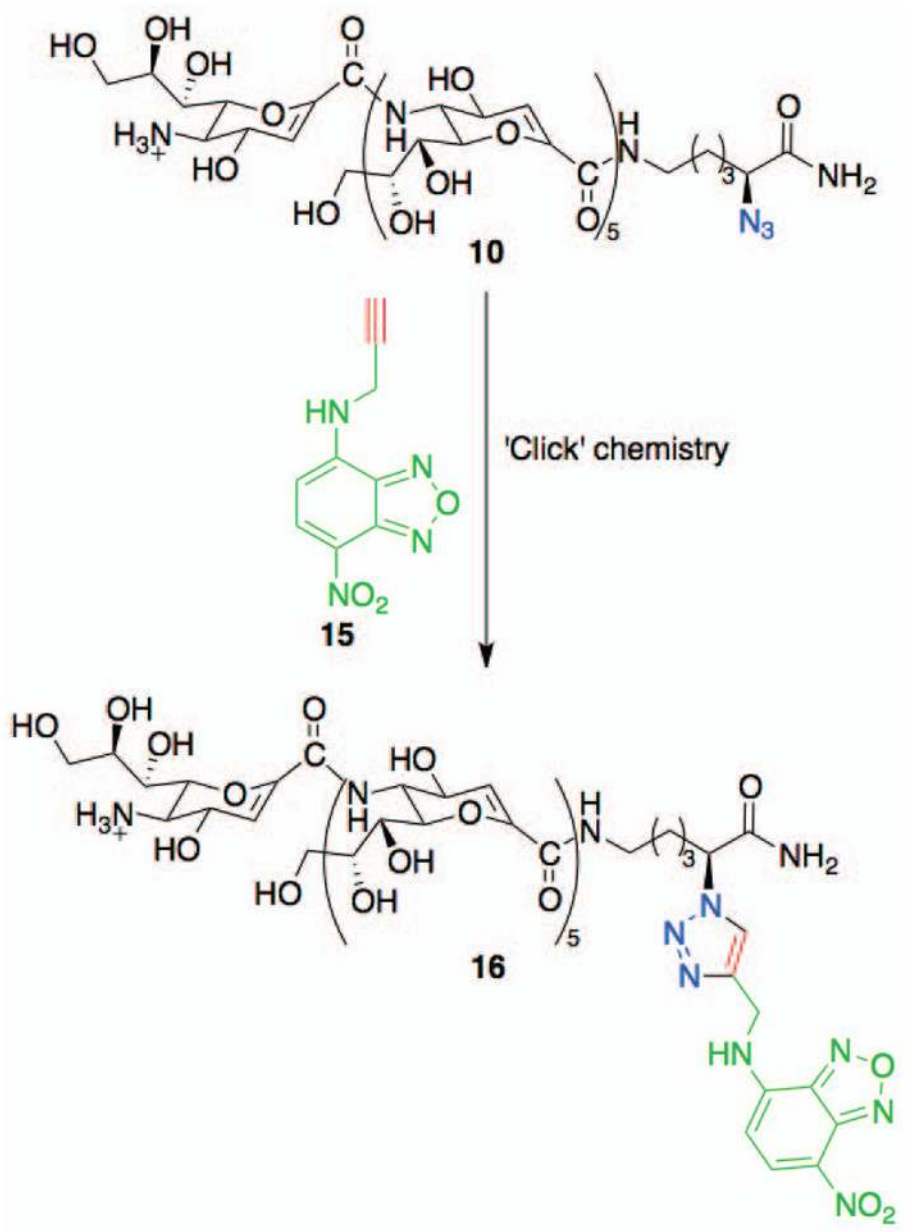

Figure 8.
Conjugation of NBD-propargylamine at the *C*-terminal azide of peptide **10** by 'Click' chemistry.

Table 1

Analyses of peak and trough of molar ellipticities of **2** – **10** at 25 °C indicate increase in 2° structure stability with length.

Compound	λmax, nm	λmin, nm	Peak, [θ]	Trough, [θ]	Peak – Trough, Δ[θ]
2	240	210	2,190	–428	2,617
3	242	212	8,263	–5,568	13,830
4	242	212	10,764	–6,733	17,497
5	241	212	11,384	–7,395	18,779
6	240	211	11,422	–7,185	18,607
7	241	211	11,376	–7,498	18,874
8	240	211	10,219	–7,420	17,639
9	241	211	13,288	–9,539	22,827
10	241	211	12,017	–7,200	19,217

Table 2

Half-life from NH/ND exchange for compounds **3** – **9**.

	3	**4**	**5**	**6**	**7**	**8**	**9**
$t_{1/2}$ linker amide, s	7.0 ± 2.2	5.8 ± 1.1	5.9 ± 1.2	6.3 ± 1.1	5.5 ± 2.9	5.1 ± 1.5	5.1 ± 2.2
$t_{1/2}$ internal Neu2en amides, s	7.1 ± 1.3	19.3 ± 4.7	16.7 ± 3.1	17.7 ± 2.8	13.6 ± 1.7	16.3 ± 3.0	16.4 ± 1.3
$t_{1/2}$ *C*-terminal Neu2en amide, s	n/a	8.5 ± 2.5	6.9 ± 1.5	7.8 ± 0.9	12.8 ± 9.6	7.6 ± 1.6	6.6 ± 0.9

Table 3

Properties of calculated lowest energy structures of **10.**

r.m.s.d. for Neu2en backbone, Å	0.982 ± 0.230
r.m.s.d. for Non-H atoms, including side chains, Å	1.912 ± 0.323
Total Number of NOEs	84
Final Energy, kcal/mol	686.873